Kinetics of Protein Foam Destabilization: Evaluation of a Method Using Bovine Serum Albumin

Myeong-Ae Yu and Srinivasan Damodaran*

Department of Food Science, University of Wisconsin—Madison, 1605 Linden Drive, Madison, Wisconsin 53706

A method to study the kinetics of protein foam decay has been evaluated. The method involves monitoring of pressure change as a function of time in a closed system containing a foam, which then is converted to decay of the interfacial area of the foam as a function of time. The method provides a means to estimate the initial surface area of foams. Studies with bovine serum albumin (BSA) foam, as a model, revealed that the instability of protein foams generally follows either monophasic or biphasic first-order kinetics. Two microscopic processes, namely, gravitational drainage and interbubble gas diffusion, are fundamentally responsible for protein foam instability. The relative magnitude of the rate constants of these two processes is affected by environmental factors such as temperature, pH, and the presence of reducing agents.

INTRODUCTION

Proteins at liquid interfaces play important roles in many biological systems and industrial product formulations. Perhaps the most important application of the interfacial properties of proteins is their use as macromolecular surfactants in food systems such as foams and emulsions. Unlike small molecular weight surfactants, proteins are able to form a continuous network of cohesive film at interfaces via complex intermolecular interactions that impart stability to the film.

Several studies have demonstrated that the foamability of proteins is fundamentally related to their ability to form films at the air–water interface (Cumper, 1953; Mita et al., 1977, 1978). Proteins that rapidly adsorb and readily undergo unfolding and molecular rearrangement at the air–water interface exhibit better foamability than those that adsorb slowly and resist unfolding at the interface (Graham and Phillips, 1976; Song and Damodaran, 1987). However, studies have also shown that proteins that have good foamability do not seem to possess molecular properties that impart stability to the foam, whereas proteins that do not possess molecular flexibility to form foam do seem to possess properties that impart stability (Graham and Phillips, 1976). Thus, it is apparent that for a protein to be a good surfactant it should possess two sets of molecular properties, one pertaining to its foamability and the other related to its stability. From the application viewpoint, while the ability of a protein to generate a foam is essential, the ability to stabilize the foam is more crucial. In this regard, the molecular mechanisms that are involved in foam stability are poorly understood.

One of the major limitations to understanding microscopic as well as macroscopic events that lead to foam collapse and the contribution of various molecular properties of the protein to these events is the lack of a reliable scientific method to study the kinetics of foam destabilization. Several methods have been used in the past to study the stability of protein foams. These include measurement of liquid drainage (Mita et al., 1977; Waniska and Kinsella, 1979; German et al., 1985), foam volume (Graham and Phillips, 1976), and conductivity of foams (Kato et al., 1983; Wright et al., 1987) and photographic techniques (Clark and Blackman, 1948; Mita et al., 1978). Among these approaches, the measurement of liquid drainage as a function of time is the most widely used because of its simplicity. However, as pointed out by Halling (1981), measurement of liquid drainage from the lamellar phase of foams provides only a crude picture of stability of foams, because it is not the sole factor but only one of the factors that is responsible for foam breakage. Furthermore, it does not provide insight into the molecular factors that are ultimately responsible for the stability or instability of protein-stabilized foams. Hence, there is a need to develop methods that are based on rigorous physical principles. In this paper, we apply such a method to study the kinetics of destabilization of protein foams. The method is based on the theoretical principles developed by Ross (1969).

THEORETICAL BACKGROUND

The equation of state of a spherical foam particle is given by the Laplace equation

$$P_i - P_e = 4\gamma/r \quad (1)$$

where P_i and P_e are the pressures inside and outside (atmospheric), respectively, of the gas bubble, r is the radius of the bubble, and γ is the surface tension. According to the Laplace equation, the pressure inside a bubble is always greater than the pressure outside. When the bubble is stable, this pressure difference is compensated by surface tension of the film. It follows then that if the bubble is contained in a closed system with constant volume, any event that leads to breakage of the bubble would increase the pressure inside the chamber. Conversely, if a foam is formed in a closed container, the rate of collapse of the foam can be monitored by measuring the rate of change of pressure in the container external to the foam.

The bubbles in a homogeneous foam are considered to have a polyhedron shape. However, in practical situations, since a foam is a polydisperse system, the bubbles in a typical foam can essentially be considered to be spherical (Ross, 1969). On the basis of the Laplace equation, the equation of state of a foam in terms of foam volume and

* To whom correspondence should be addressed.

0021-8561/91/1439-1555$02.50/0

interfacial area can be derived as follows (Ross, 1969; Nishioka, 1986): The total volume of a polydisperse foam can be expressed as

$$V_f = a_1 r_1^3 + a_2 r_2^3 + a_3 r_3^3 + \ldots + a_i r_i^3 = \sum_i a_i r_1^3 \quad (2)$$

where r_i is the radius of the ith bubble in the polydisperse foam and a_i is a constant. Similarly, the total interfacial area of a foam can be expressed as

$$A_f = b_1 r_1^2 + b_2 r_2^2 + b_3 r_2^2 + \ldots + b_i r_2^2 = \sum b_i r_1^2 \quad (3)$$

where b_i is a constant. If foam decays at constant external pressure, the volume of the gas will increase, whereas the surface area of the foam will decrease. However, at equilibrium, when there is no net breakage or formation of bubbles, the free energy arising from the pressure difference across the film (which tends to expand the film), i.e., $(P_i - P_e)\,dv$, is quantitatively compensated by the increase in surface free energy, $\gamma\,dA$, that would result from the creation of new surface area of the bubble. That is

$$(P_i - P_e)\,dv = \gamma\,dA \quad (4)$$

Substituting for the volume and surface area of a single foam cell as $V = ar^3$ and $A = br^2$, respectively, and taking into consideration that a single foam cell has internal and external surface areas, it can be shown that the ratio of the constants a to b is given by $a = b/6$. Assuming that the system obeys ideal gas law, the total amount of gas inside the foam, n_f, can be expressed as

$$n_f = \sum (P_i V_i)/RT \quad (5)$$

where $P_i = P_e + 4\gamma/r_i$. Therefore

$$n_f = \sum (P_e + 4\gamma/r_i)(a_i r_i^3)/RT \quad (6)$$

On simplification and substituting $a_i = b_i/6$, it can be shown that

$$n_f RT = P_e V_f + (2\gamma A/3) \quad (7)$$

Equation 7 is the equation of state for a foam (Ross, 1969).

Nishioka and Ross (1981) further developed this relationship to relate the pressure change external to a foam in a vessel of constant volume and temperature to changes in its interfacial area during foam decay. Briefly, if n_e is the quantity of gas external to the foam, then the total quantity of gas in a container containing the foam at constant temperature is

$$n_e + n_f = \frac{P_e V_e}{RT} + \frac{(P_e V_f + 2/3\gamma A)}{RT} \quad (8)$$

where P_e and V_e are the pressure and volume of gas external to the foam. As the foam decays, the P_e, V_e, V_f, and A of the foam change. Then, at any time t during the decay process

$$n_e' + n_f' = \frac{P_e' V_e'}{RT} + \frac{(P_e' V_f' + 2/3\gamma A')}{RT} \quad (9)$$

Since the total quantity of gas in the closed system is constant, $n_e + n_f = n_e' + n_f'$. Therefore, from combining eqs 8 and 9 and on simplification

$$3V\Delta P + 2\gamma\Delta A = 0 \quad (10)$$

where $V = V_e + V_f = V_e' + V_f'$; $\Delta P = P_e' - P_e$ and $\Delta A = A' - A$.

The interfacial area of the foam at time t during the decay process is given by

$$A_t = A_0 + \Delta A = A_0 - \frac{3V\Delta P_t}{2\gamma} \quad (11)$$

where A_0 is the interfacial area at time $t = 0$. When the foam completely collapses at infinite time, the interfacial area becomes zero. Therefore

$$A_\infty = 0 = A_0 - \frac{3V\Delta P_\infty}{2\gamma} \quad (12)$$

or

$$A_0 = \frac{3V\Delta P_\infty}{2\gamma} \quad (13)$$

Therefore, substituting eq 13 in eq 11

$$A_t = \frac{3V}{2\gamma}(\Delta P_\infty - \Delta P_t) \quad (14)$$

Equation 14 is the relationship that describes the time-dependent changes in the interfacial area of the foam to changes in the gas pressure external to the foam. In other words, the rate of decay of a foam can be determined experimentally by measuring the rate of change of pressure external to the foam.

MATERIALS AND METHODS

Bovine serum albumin (BSA) (fraction V), dithiothreitol, and an antifoaming agent were obtained from Sigma Chemical Co. Prepurified nitrogen gas was used without further water saturation. RBS 35 detergent was obtained from Pierce Chemicals.

Protein solutions were made in 20 mM sodium phosphate buffer, pH 7.0. In experiments designed to study the effect of pH, protein solutions were prepared with distilled and deionized water instead of phosphate buffer and were adjusted to the required pH by using either HCl or NaOH. The concentration of BSA was determined by using an $E^{1\%}$ value of 6.67 at 279 nm.

Apparatus for Measuring Foam Stability. Schematic diagrams of two experimental apparatuses used in this study are shown in Figure 1. The only difference between the two systems was that the reference pressure of the differential pressure transducer was different: In the first system (Figure 1A), the reference pressure was the pressure of water-saturated nitrogen gas in a reference column identical with that of the experimental foam column. In the second system (Figure 1B), the atmospheric pressure was used as the reference pressure. Preliminary experiments showed no significant difference in the rate of decay of a foam as measured by these two systems. On the basis of this evidence, the second system (Figure 1B) was used for all the experiments, except those for the temperature effect on foam stability.

The essential features of the apparatus were as follows: It consisted of a water-jacketed column, a protein solution chamber connected to the bottom of the column by using a ground glass fitting, a fritted glass tube to bubble nitrogen gas through the protein solution, a bent glass side tube at the top of the column for storing an antifoaming agent, a glass/metal assembly containing the differential pressure transducer connected to the top of the column, and a side valve. The input of the pressure transducer (Kulite Semiconductor; XCS-190-SD, sensitivity range 0–5 psi; output 25.04 mv/psi) was connected to a 10-V dc power supply, and the output was connected to a strip chart recorder (Kipp & Zonnen). The bottom of the fritted glass tube was connected to a nitrogen gas cylinder through two flow meters (Gilmont Instruments, Inc.; F-1100 and J3227-00) connected in series. Use of two flow meters instead of one provided a better and accurate control of nitrogen flow rate. All glass connections were made with ground glass to prevent any gas leakage.

In a typical experiment, 20 mL of protein solution (1% w/v) pre-equilibrated at the experimental temperature was taken in the solution chamber. The chamber was connected to the bottom of the column. The water jacket was connected to a circulating water bath, 1 mL of the antifoaming agent (200 ppm) was placed in the bent side tube, the valve at the top of the apparatus was kept open to the atmosphere, and the reference tube of the differential pressure transducer was kept open to the atmosphere.

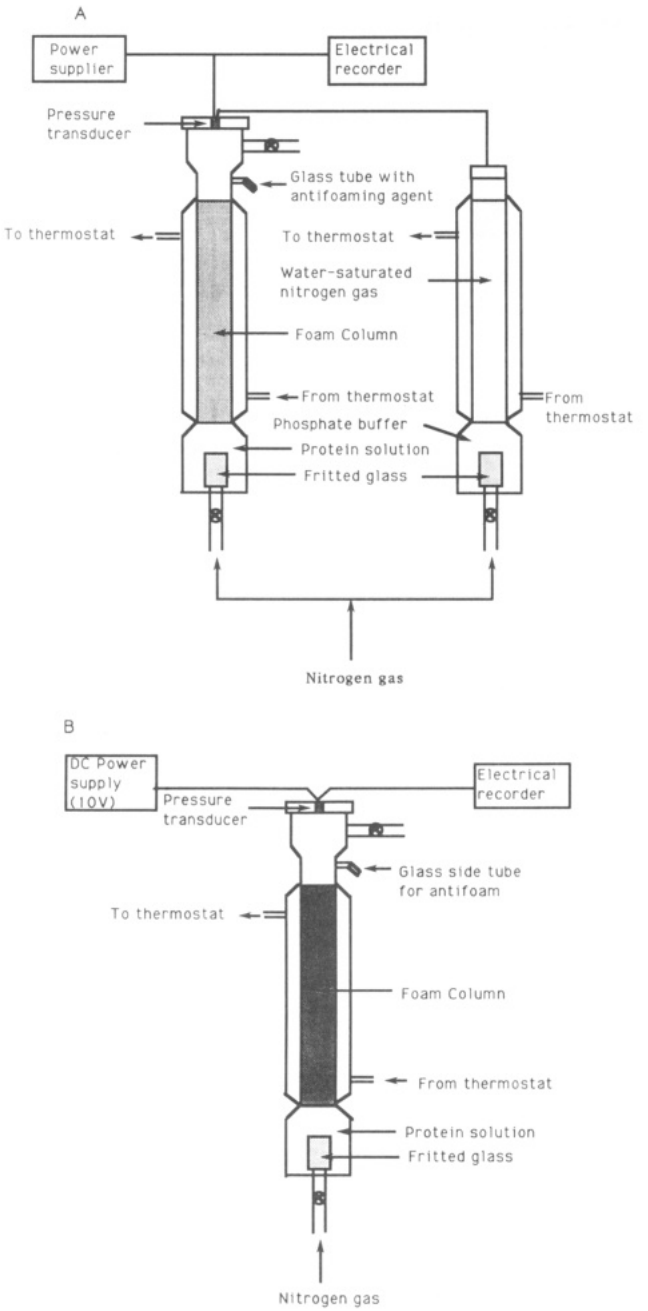

Figure 1. Schematic diagrams of the foam apparatuses used in this study.

Prepurified nitrogen gas was bubbled through the protein solution at a rate of 20.8 mL/min. Bubbling was continued until the foam rose to a premarked point at the top of the column at which time the valve at the bottom of the fritted glass tube was closed. The total volume up to the mark was 77 mL. After a brief interval of about 30 s, the valve at the top of the column was also closed. The change in the pressure at the head space of the foam was continuously recorded on the strip chart recorder. When the rate of change in the pressure approached a plateau, the antifoaming agent in the bent side tube was dropped into the column by turning the side tube through 180°. The final pressure difference (ΔP_∞) was recorded. The experiment was repeated at least three times for each test protein solution. Between experiments the apparatus was disassembled, and all glass parts (except the chamber housing the pressure transducer) were soaked in a detergent solution (RBS35 detergent) for 1 h, scrubbed and rinsed thoroughly first with water and then with acetone, and finally dried in an oven. Extreme measures were taken to ensure that no residual detergent was present in the apparatus before an experiment.

Surface Tension. Surface tension of protein solutions was measured by the Whilhelmy plate method using an electrobalance (Cahn Instruments) as described elsewhere (Song and Damodaran, 1987).

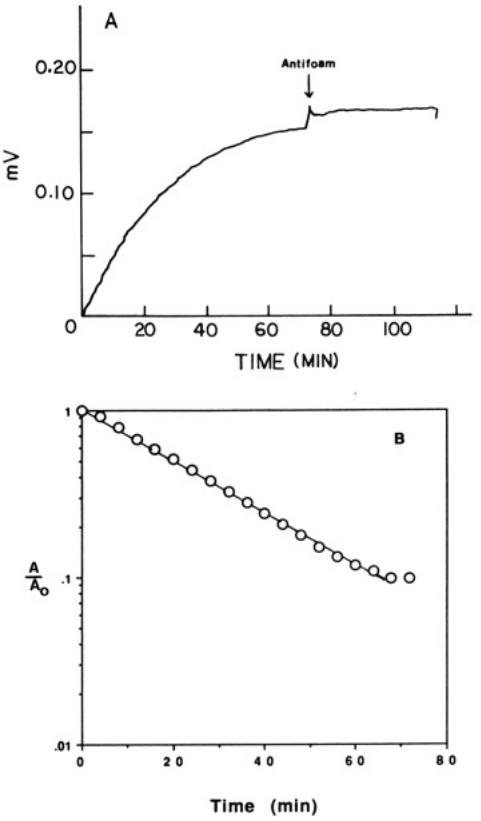

Figure 2. (A) Typical recorder tracing of the pressure change as a function of time inside the foam apparatus containing a BSA foam (1% BSA, pH 7.0, 25 °C). 25.04 mV = 1 psi. (B) First-order plot of the decay of BSA foam.

RESULTS AND DISCUSSION

A typical recorder tracing of the pressure change as a function of time inside the foam apparatus containing a BSA-stabilized foam is shown in Figue 2A. The pressure inside the foam apparatus increased with time and reached a plateau after about 60 min. When the antifoaming agent was added at 80 min, collapse of the remaining foam in the column occurred. This caused a sharp increase in the inside pressure, followed by attainment of a final value. The final change in the pressure was taken as the net pressure change, ΔP_∞, that would have resulted if the foam collapsed completely at infinite time.

The total initial interfacial area of the foam, A_0, was calculated from ΔP_∞ by using eq 13. A dimensionless fractional interfacial area at any given time t during foam decay was calculated by using the relation

$$A/A_0 = (\Delta P_\infty - \Delta P_t)/\Delta P_\infty \qquad (15)$$

The plot of fractional area A/A_0 against time for the BSA-stabilized foam is shown in Figure 2B.

Kinetic analyses of foam stability based on liquid drainage measurements have shown that while the stability of certain protein foams, e.g., wheat gluten, follow first-order kinetics (Mita et al., 1977), other protein foams, e.g., caseins (Halling, 1981) and phosphorylated yeast protein (Huang and Kinsella, 1987), follow second-order kinetics. However, the rate of decay of BSA foam measured by using the method described here did not fit either first-order or second-order kinetics.

In phenomenological terms, decay of a foam expressed in terms of surface area decay can be assumed to follow multiphasic first-order kinetics, which can be expressed

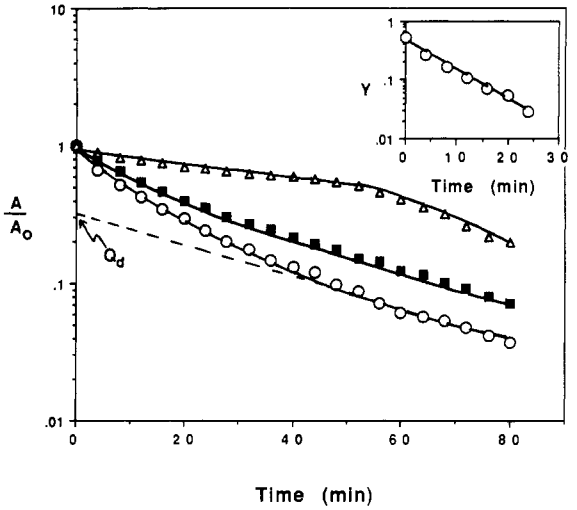

Figure 3. Surface area decay of BSA foams under various experimental conditions [(○) pH 4.0; (■) pH 7.0; (△) pH 7.0] and in the presence of 5.0 mM dithiothreitol. The inset is the semilog plot of the residue Y as a function of time (see text for details) for the BSA foam at pH 4.0. The protein concentration in all cases was 1.0%.

as

$$A_t/A_0 = Q_1 \exp(-k_1 t) + Q_2 \exp(-k_2 t) + \ldots Q_i \exp(-k_i t) + \ldots \quad (16)$$

where k_i is the macroscopic rate constant of the ith first-order kinetic phase and Q_i is the amplitude parameter of the ith kinetic phase. Monophasic first-order kinetics would involve only one exponential term and biphasic first-order would involve two exponential terms.

Analysis of the decay of BSA foams according to first-order kinetics indicated that, depending upon the experimental conditions, the decay process followed either monophasic or biphasic first-order kinetics within the time scale (i.e., 0–80 min) studied. For example, while decay of BSA foam exhibited monophasic first order at pH 7.0, it followed biphasic first order at pH 4.0 and at pH 7.0 in the presence of 5.0 mM DTT (Figure 3). The biphasic first-order kinetics indicate that two microscopic processes might be involved in the foam decay process. These two processes might be the gravitational drainage of liquid from the lamella and disproportionation of gas bubbles via interbubble gas diffusion (Monsalve and Schechter, 1984). Since gravitational drainage and gas diffusion across bubbles are the major causes of foam breakage (Damodaran, 1990), it is logical to expect that these two processes must occur during the decay of any foam under all conditions, irrespective of whether the kinetics exhibit biphasic or monophasic first order. In other words, the decay of a foam should conform to the relationship

$$A_t/A_0 = Q_g \exp(-k_g t) + Q_d \exp(-k_d t) \quad (17)$$

where k_g and k_d are first-order rate constants for the gravitational drainage and gas diffusion processes, respectively. While the existence of these two microscopic processes is self-evident in biphasic first-order behavior, in systems that exhibit monophasic first-order kinetics, the rate constants k_g and k_d might be equal in magnitude and these processes might occur simultaneously. Furthermore, since the magnitude of foam decay by interbubble gas diffusion is significant only below a critical film thickness, it is reasonable to attribute the first kinetic phase observed in a nonlinear first-order plot to the gravitational drainage process.

In the case of nonlinear first-order plots, the rate constants k_g and k_d were determined according to the exponent "stripping" procedure (Ikai et al., 1973; Monsalve and Schechter, 1984). According to this approach, the rate constant of the last first-order kinetic region (i.e., the rate-limiting step) is obtained from the slope of the last linear region (in this case, the second linear region) and the amplitude parameter Q_d is obtained from the intercept, as shown in Figure 3. Then, the term $Q_d \exp(-k_d t)$ is subtracted from the left-hand side of eq 17. The logarithm of the residue (Y) is then plotted against time as shown in Figure 3 (inset). The values of k_g and Q_g are then calculated from the slope and the intercept, respectively, of this plot. Since the boundary conditions of eq 17 are 1 and 0 at times t_0 and t_∞, respectively, it follows that $Q_g + Q_d = 1$.

It should be pointed out that the above method of analysis is appropriate only for systems that exhibit concave-type first-order kinetics. For systems that exhibit convex-type nonlinear first-order kinetics, such as the behavior of BSA foam at pH 7.0 in the presence of 5.0 mM DTT, the above method of analysis would be inappropriate, because in such systems the first kinetic phase is the rate-limiting step and the condition that $Q_g + Q_d = 1$ cannot be satisfied. In these instances it would be more appropriate to obtain the rate constants directly from the slopes of the two linear regions of the plot.

The initial surface area of the foam was calculated by using eq 13. Since the same volume of foam was formed in all experiments, A_0 can be defined as foaming activity index (FAI), which reflects the amount of interfacial area created by a protein under a given set of foaming conditions. The greater the value of A_0, the greater would be the foaming activity of the protein.

Bovine serum albumin is known to be a good foaming agent. It was chosen as a model protein for this study since its molecular characteristics are well-known (Haurowitz, 1963; Brown, 1977; Foster, 1977). The conformation of BSA is significantly altered by environmental conditions and by additives such as denaturants, reductants, etc. Changes in the properties and conformation of BSA can cause dramatic changes in its foaming properties. Three important factors, namely, temperature, pH, and cleavage of disulfide bonds, which influence the conformation of BSA were systematically investigated.

Effect of Temperature on BSA Foam. The values of initial surface area, A_0, of BSA foam at various temperatures are presented in Table I. A_0 increased with temperature, indicating that the mean size of bubbles was smaller at higher temperatures and larger at lower temperatures (since the volume of the foam formed was the same). Using a photographic method, Mita et al. (1978) reported that the bubble size of gluten foam decreased with rising temperature. The authors attributed this to a lowering of surface tension and bulk viscosity as the temperature was raised. The mobility of protein molecules increases as viscosity of the lamella fluid is decreased by rising temperature. This facilitates increased molecular diffusion and enhances protein adsorption at the air–water interface. In addition, partial denaturation of protein molecules at high temperature increases molecular flexibility; this in turn increases the probability that a greater number of protein segments will adsorb at the interface. These molecular events, which increase the surface activity

Table I. Initial Surface Area, A_0, of BSA Foam (1.0%, pH 7.0) at Various Temperatures

temp, °C	$A_0 \times 10^{-3}$, cm^2	temp, °C	$A_0 \times 10^{-3}$, cm^2
15	23.6 ± 0.9	30	30.3 ± 1.7
20	23.2 ± 0.5	40	45.3 ± 1.6
25	26.8 ± 1.0		

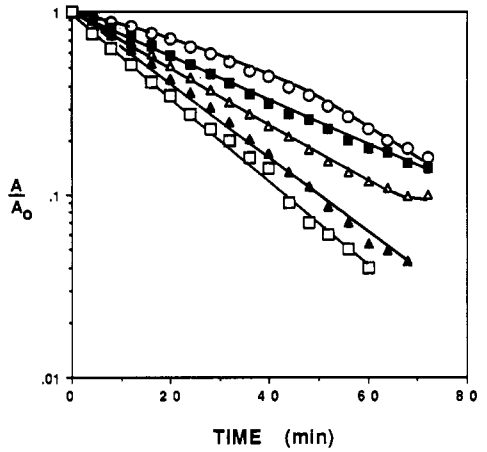

Figure 4. Surface area decay of BSA foams (1%, pH 7.0) at various temperatures: (○) 15 °C; (■) 20 °C; (△) 25 °C; (▲) 30 °C; (□) 40 °C.

of the protein molecule, might be responsible for smaller mean bubble size at high temperatures.

In contrast to the positive influence of temperature on the foamability (i.e., FAI) of BSA, the stability of BSA foam was adversely affected by temperature. The rate of surface area decay increased as the temperature was increased (Figure 4). Of the temperatures studied, BSA foam was most stable at 15 °C. The reduced stability at higher temperature might be due to a decrease in bulk viscosity. While the decrease in bulk viscosity at high temperature facilitates rapid adsorption, unfolding, and creation of large interfacial area (A_0), the same decrease in bulk viscosity as well as the decreased film viscosity seems to promote gravitational drainage and increased gas diffusion across bubbles. Both of these events would lead to foam destabilization. In a simple solution, the viscosity as a function of temperature can be expressed by an Arrhenius-type equation

$$\eta = \exp(A + B/T) \tag{18}$$

where A and B are constants and T is absolute temperature (Rha and Pradipasena, 1986). Since the drainage rate is inversely proportional to η (Hanson and Derderial, 1976), the increase in viscosity at low temperature would retard the rate of drainage, although at the same time it would also decrease the foam volume by lowering the rate of protein adsorption and film formation during bubbling. Similarly, viscosity of the protein film, η_s, also may play a role in improving foam stability against liquid drainage. Oortwijn and Walstra (1979) reported that the surface viscosity of adsorbed protein films increased as the temperature was lowered. The rate of thermal and interfacial denaturation of proteins also tends to be minimized at low temperature. Therefore, the tendency of protein coagulation/precipitation at the interface is also minimized at low temperature. Furthermore, polar interactions between the adsorbed molecules, such as electrostatic repulsion, hydrogen-bonding interaction, and hydration forces, become dominant at low temperature. These interactions, along with steric repulsion, greatly retard the rate of drainage of the lamella fluid. On the other hand, at high temperature, partial denaturation/unfolding of the protein at the interface may lead to aggregation and precipitation; this may enhance liquid drainage by lowering the viscosity and destabilize the integrity of the film.

The decay of BSA foam exhibited biphasic first-order kinetics at 15 °C, whereas at higher temperatures it essentially followed monophasic first-order kinetics within the time scale studied. As mentioned earlier, even though monophasic first order was observed at 20–40 °C, it is only logical to assume that both gravitational drainage and gas diffusion processes were involved.

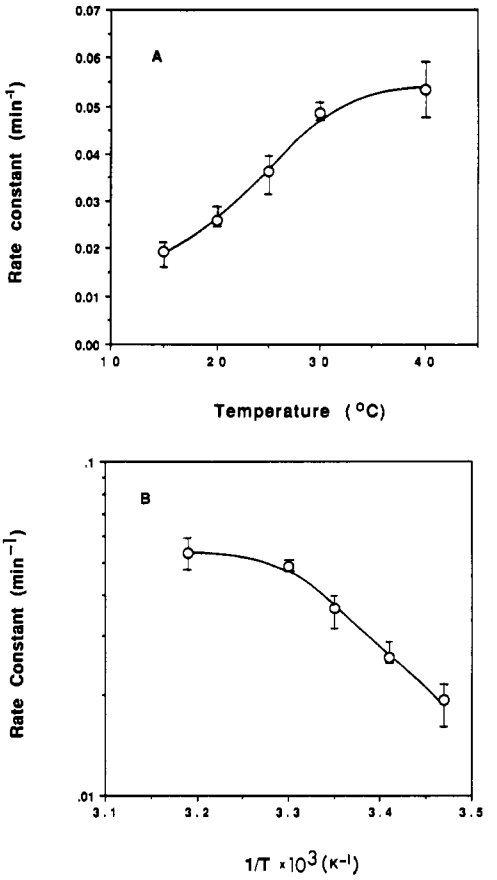

Figure 5. (A) Effect of temperature on the first-order rate constant of decay of BSA foam (1%, pH 7.0). (B) Arrhenius plot of the data.

Table II. Initial Surface Area, A_0, of BSA Foam (1.0%, 25 °C) at Various pHs

pH	$A_0 \times 10^{-3}$, cm²	pH	$A_0 \times 10^{-3}$, cm²
4.0	20.4 ± 3.4	6.0	23.0 ± 0.8
4.5	44.5 ± 0.6	7.0	32.0 ± 2.8
5.0	60.2 ± 1.9		

The relationship between first-order rate constant and temperature is shown in Figure 5A. The datum point for 15 °C represents the gravitational drainage rate constant obtained from the slope of the first kinetic phase. The rate constant vs temperature plot exhibited a sigmoidal behavior. The Arrhenius plot is curvilinear (Figure 5B), which could be divided into two linear regions. The bilinear Arrhenius plot indicates that two activation energies corresponding to two molecular processes are involved in the decay process. The activation energy calculated for the 15–30 °C range is about 10.9 kcal/mol, while that for the 30–40 °C range is about 1.8 kcal/mol. The higher activation energy required at 15–30 °C might be related to higher viscosity as well as enhanced hydrogen bonding and ion–dipole interaction of water with the polar functional groups of protein which might decrease the gravitational drainage rate. The lower activation energy for the 30–40 °C range might relate to weakening of these interactions and an increase in the gas diffusion across bubbles.

Effect of pH. Values for the initial surface area of BSA stabilized foam at various pHs are presented in Table II. The value of A_0 exhibited a maximum at or near the isoelectric pH (5.3) of BSA, indicating that bubble size was the smallest near the isoelectric pH. This is expected, because electrostatic repulsion between adsorbed proteins

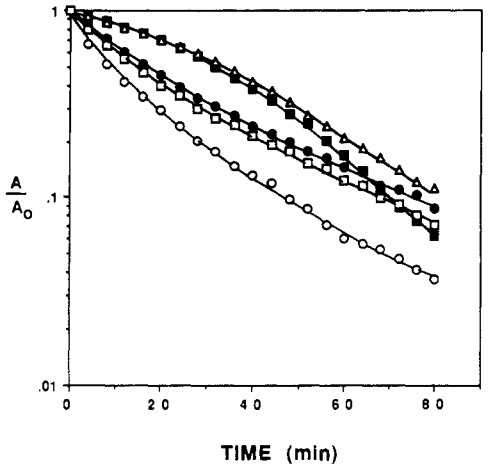

Figure 6. Surface area decay of BSA foam (1% at 25 °C) at various pHs: (○) pH 4.0; (■) pH 4.5; (△) pH 5.0; (●) pH 6.0; (□) pH 7.0.

and protein molecules approaching the interface would be minimum at or near the isoelectric pH. Furthermore, the lack of electrostatic repulsion between molecules at the interface might facilitate formation of a cohesive viscous protein film (Bacon et al., 1988). Mussellwhite (1967) reported that the thickness of BSA film at the air–water interface increased as the pH approached its p*I*.

The rate of foam decay at various pHs is shown in Figure 6. The overall stability of BSA foam was higher at or near its isoelectric pH (pH 4.5 and 5.0) and decreased as the pH was shifted away from the p*I*. Several investigators have reported that the stability of protein-stabilized foams is maximum at or near p*I* of proteins, provided there is no loss of solubility (Cumper, 1953; Buckingham, 1970; Graham and Phillips, 1976; Mita et al., 1977; Waniska and Kinsella, 1979). In the region of the isoelectric point electrostatic repulsion is least since the net charge of the protein is zero. Therefore, cohesive interaction between protein molecules in the film via noncovalent forces is greatest near the p*I*. This improves the mechanical properties of the film and thus foam stability. It has been shown that the mechanical properties of adsorbed protein films increase and are maximized as the pH approaches the p*I* (Mita et al., 1977; Graham and Phillips, 1980; Phillips, 1981; Kim and Kinsella, 1985). The high surface viscosity of the film retards lamella drainage (Mita et al., 1977). The surface yield stress and elasticity of protein films are maximum near the p*I* (Graham and Phillips, 1980). According to Kim and Kinsella (1985), the surface viscosity, surface yield stress, and film elasticity showed maximum in the range pH 5.0–6.0, and the stability of BSA foam was maximum in the same pH range.

At pH 4.5 and 5.0 the nonlinear first-order plots of BSA foam decay were convex in shape, whereas at pH 4.0, 6.0, and 7.0, they were concave in shape. The concave shape of the curves at pH 4.0, 6.0, and 7.0 indicates that the rate of decay due to gravitational drainage is greater than that due to gas diffusion. In other words, gravitational drainage is not the rate-limiting step for foam decay at these pH. This suggests that both gravitational drainage and gas diffusion processes might occur simultaneously and thus accelerate decay of the foam. In contrast, the convex shape of curves at pH 4.5 and 5.0 indicates that the rate of foam decay due to gravitational drainage is slower than that due to gas diffusion. However, since interbubble gas diffusion cannot be significant above a critical thickness of the lamella, a critical amount of initial liquid drainage and film thinning is essential for gas diffusion to commence. In other words, in a convex-shaped decaying system, the

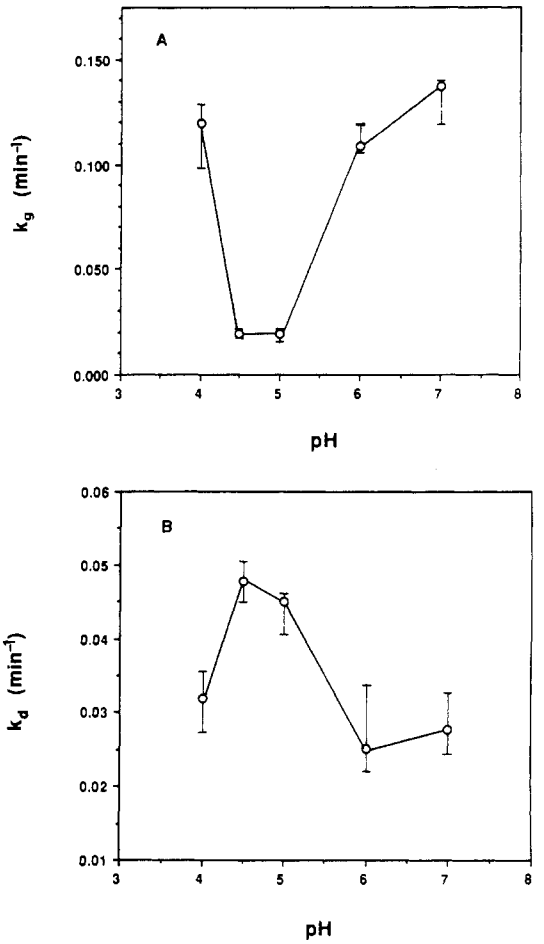

Figure 7. (A) Effect of pH on the rate constant of decay due to gravitational liquid drainage, k_g, and (B) interbubble gas diffusion, k_d.

first phase is purely related to the gravitational drainage process and it is the rate-limiting step in the overall decay process.

The effect of pH on the gravitational drainage rate constant, k_g, is shown in Figure 7A. The k_g was minimal at pH 4.5–5.0. Above and below this pH range, k_g increased dramatically. The relationship between the gas diffusion rate constant and pH is shown in Figure 7B. In contrast to k_g, the k_d exhibited a maximum at pH 4.5 and a minimum at pH 6.0–7.0. The seemingly contradictory behavior of k_g and k_d as a function of pH may be explained as follows: At pH 4.5–5.0, which is near the isoelectric pH of the protein, the decreased electrostatic repulsion between the protein molecules in the film, the greater extent of protein adsorption, and favorable intermolecular interactions between the adsorbed molecules create a highly viscous protein film that dramatically retards drainage of lamellar fluid by hydrostatic and gravitational forces. However, once the lamella approaches a critical thickness due to liquid drainage, the lack of electrostatic repulsion and the proximity of the protein films on either side of the lamella promote attractive interactions, such as van der Waals and hydrophobic interactions, between the protein films. This might lead to coagulation and precipitation of the adsorbed proteins which in turn might create "holes" in the lamella film and thus enhance the rate of gas diffusion across the bubbles. On the other hand, at pH 4.0, 6.0, and 7.0, far from the isoelectric pH of the protein, electrostatic repulsion between protein molecules within the film as well as between the films would adversely affect formation of a highly cohesive viscous film. Such a film may not have the ability to retard the rate of initial liquid drainage due to hydrostatic and gravitational forces. However,

Table III. Effect of Disulfide Bond Cleavage at Various Levels on the Initial Surface Area of BSA Foam (2.0%, pH 7.0) at 25 °C

concn of DTT, mM	$A_0 \times 10^{-3}$, cm^2	concn of DTT, mM	$A_0 \times 10^{-3}$, cm^2
0.0	26.8 ± 3.5	5.0	27.2 ± 8.9
0.5	32.0 ± 2.6	10.0	26.7 ± 3.4
1.0	29.8 ± 3.8		

when the lamella approaches a critical thickness, the electrostatic repulsion between the protein films on either side of the lamella would retard further drainage of the lamella and also prevent coagulation of the protein and formation of holes in the lamella. These events would maintain the rate of gas diffusion across the bubbles at a lower rate compared to that at pH 4.5–5.0.

Effect of Disulfide Bond Cleavage. The ability of a protein to unfold at the interface determines the extent of its adsorption and, therefore, the foaming behavior of the protein. Proteins that unfold more at the interface are more surface active (Graham and Phillips, 1979). Globular proteins like lysozyme and BSA, which have intramolecular disulfide bonds, exhibit lesser surface activity than random coil proteins such as β-casein. Therefore, cleavage of disulfide bonds in proteins, which induces conformational change and increases molecular flexibility, may affect the interfacial behavior of proteins very significantly. The effect of S–S bond cleavage on the foaming behavior of BSA was tested in this study.

The values of initial surface area, A_0, of BSA foam formed in the presence of dithiothreitol (DTT) at various concentrations are presented in Table III. The A_0 value was significantly larger at 0.5 mM DTT than at other concentrations. It is generally believed that because of high flexibility and lack of intramolecular constraints, a highly unfolded protein would occupy a greater surface area at the interface and thus would be able to generate more interfacial area under a given set of foaming conditions. However, the data presented in Table III do not support this view, because at 10 mM DTT concentration, which should have cleaved all 17 disulfide bonds in BSA, the total initial surface area of the foam was actually less than that at 0.5 mM DTT, which would have cleaved only a limited number of disulfide bonds. The data suggest that the critical number of disulfide bonds broken at 0.5 mM DTT produces an intermediate structure of BSA that seems to have greater surface activity than the conformational states of BSA that are produced at other DTT concentrations. This implies that for a protein to possess better foaming activity it should possess an optimum amount of molecular flexibility/rigidity; neither the tightly folded rigid structure nor the completely unfolded flexible structure seems to have the ability to impart better foaming activity to the protein. Similar conclusions have been reached in a previous study on the adsorption of structural intermediates of BSA at the air–water interface (Song and Damodaran, 1987; Damodaran and Song, 1988).

The kinetics of surface area decay of BSA foam formed in the presence of DTT at various concentrations are shown in Figure 8. The stability of BSA foam increased as the concentration of DTT was increased from 0 to 10 mM. This is in contrast to the behavior of A_0, which showed a maximum at 0.5 mM DTT. The improved foam stability at higher DTT concentrations may be attributed to cleavage of a maximum number of disulfide bonds and extensive changes in the conformation of the protein. The increase in the hydrodynamic radius of the protein and the exposure of hydrophobic residues which were buried in the native protein may increase film viscosity and

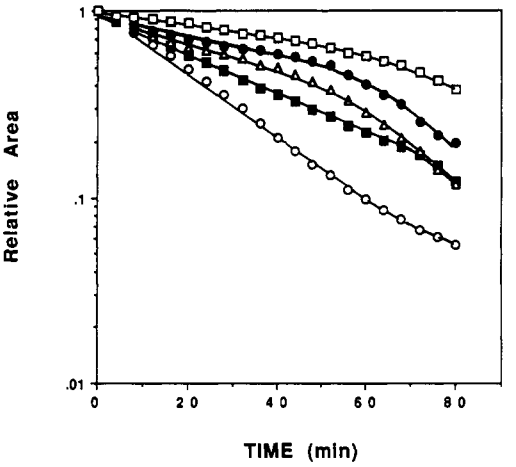

Figure 8. Effect of DTT concentration on the surface area decay of BSA foam (1%, pH 7.0) at 25 °C: (○) 0 mM; (■) 0.5 mM; (△) 1.0 mM; (●) 5.0 mM; (□) 10.0 mM.

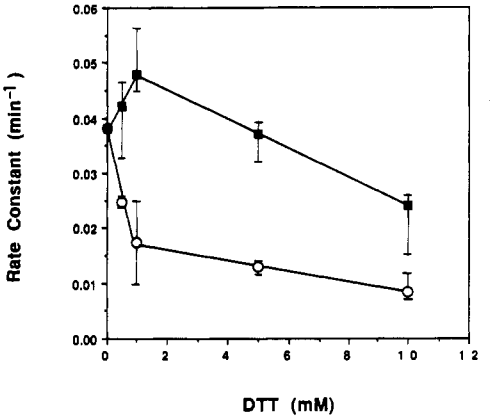

Figure 9. Effect of DTT concentration on the liquid drainage rate constant, k_g (○), and the gas diffusion rate constant, k_d (■).

facilitate formation of a cohesive film at higher DTT concentrations. However, it should be emphasized that the conditions that impart better stability to the foam do not necessarily seem to impart better foaming activity.

The shape of the surface area decay curves was affected by DTT concentration. At 0 and 0.5 mM DTT concentrations, the first-order curve was essentially monophasic up to 70 min, indicating gravitational drainage and gas diffusion rate constants were of the same magnitude. However, above 0.5 mM DTT concentration, the first-order curves were convex in nature, indicating that the foam was more stable against gravitational drainage. These results clearly indicate that the relative magnitudes of various microscopic processes that cause decay of a protein foam are very much affected by the physicochemical and structural states of the protein at the interface.

The effects of DTT concentration on the gravitational rate constant k_g and the gas diffusion rate constant k_d are shown in Figure 9. The value of k_g dropped precipitously at 1.0 mM DTT and continued to decrease gradually up to 10 mM DTT. This suggests that the number of disulfide bonds that are broken at 1.0 mM DTT concentration and the extent of conformational change that occurs in BSA as a result seem to have a major effect on the ability of the protein to form a cohesive film. In contrast to the behavior of k_g, k_d increased slightly at 1.0 mM DTT concentration and then decreased sharply as the DTT concentration was increased to 10.0 mM. The net increase in k_d at 1.0 mM DTT, however, was much smaller than the net decrease in k_g at 1.0 mM DTT. The data in Figure 9 show that both liquid drainage and interbubble gas diffusion are retarded when the disulfide bonds in BSA

are cleaved by DTT. This clearly suggests that removal of molecular constraints imposed by disulfide bonds may generally improve the stability of protein foams.

CONCLUSIONS

The method described here to study the kinetics of foam decay provides more fundamental information on the microscopic processes that cause decay of protein foams. The method is highly sensitive and is adaptable to a variety of experimental conditions. The method also provides a means to estimate the initial surface area of foams, which may be regarded as the foaming activity index (FAI) of a protein under a given set of foaming conditions. It should also be emphasized that the rate of decay of interfacial area is a more fundamental measure of the stability of foam than the rate of liquid drainage.

It is shown that the kinetics of destabilization of protein foams generally follow biphasic first order: The initial phase of the decay process is related to gravitational drainage of the lamella fluid, and the second phase is related to gas diffusion across bubbles. The rates of these two fundamental processes are dependent upon the conformational properties of proteins as well as rheological properties of the protein film and the lamella fluid. More research, however, is needed to establish these relationships.

ACKNOWLEDGMENT

Support in part from the National Science Foundation (Grant BCS 8913053) is gratefully acknowledged.

LITERATURE CITED

Bacon, J. R.; Hemmant, J. W.; Lambert, N.; Moore, R.; Wright, D. J. Characterization of the foaming properties of lysozymes and α-lactalbumins: A structural evaluation. *Food Hydrocolloids* **1988**, *2*, 224–245.

Brown, J. R. Serum albumin: Amino acid sequence. In *Albumin: Structure, Function and Uses*; Rosenoer, V. M., Oratz, M., Rothschild, M. A., Eds.; Pergamon Press: New York, 1977; pp 27–51.

Buckingham, J. H. Effect of pH, concentration, and temperature on the strength of cytoplasmic protein foams. *J. Sci. Food Agric.* **1970**, *21*, 441–445.

Clark, N. O.; Blackman, M. The transmission of light through foam. *Trans. Faraday Soc.* **1948**, *44*, 7–13.

Cumper, C. W. N. The stabilization of foams by proteins. *Trans. Faraday Soc.* **1953**, *49*, 1360–1369.

Damodaran, S. Interfaces, protein films, and foams. *Adv. Food Nutr. Res.* **1990**, *34*, 1–79.

Damodaran, S.; Song, K. B. Kinetics of adsorption of proteins at interfaces: role of protein conformation in diffusion adsorption. *Biochim. Biophys. Acta* **1988**, *954*, 253–264.

Foster, J. F. Some aspects of the structure and conformational properties of serum albumin. In *Albumin Structure, Function and Uses*; Rosenoer, V. M., Oratz, M., Rothschild, M. A., Eds.; Pergamon Press: New York, 1977; pp 53–84.

German, J. B.; O'Neil, T. E.; Kinsella, J. E. Film forming and foaming behavior of food proteins. *J. Am. Oil Chem. Soc.* **1985**, *62*, 1358–1366.

Graham, D. E.; Phillips, M. C. The conformation of proteins at the air-water interface and their role in stabilizing foams. In *Foams*; Akers, R. J., Ed.; Academic Press: New York, 1976; pp 237–255.

Graham, D. E.; Phillips, M. C. Proteins at liquid interfaces: III. Molecular structures of adsorbed films. *J. Colloid Interface Sci.* **1979**, *70*, 427–459.

Graham, D. E.; Phillips, M. C. Proteins at liquid interfaces: IV. Dilatational properties. *J. Colloid Interface Sci.* **1980**, *76*, 227–239.

Halling, P. J. Protein-stabilized foams and emulsions. *CRC Crit. Rev. Food Sci. Nutr.* **1981**, *15*, 155–203.

Hansen, R. S.; Derderian, E. J. Problems in foam origin, drainage and rupture. In *Foams*; Akers, R. J., Ed.; Academic Press: New York, 1976; pp 1–14.

Haurowitz, F. *The chemistry and function of proteins*; Academic Press: New York, 1963; p 184.

Huang, Y. T.; Kinsella, J. E. Effects of phosphorylation on emulsifying and foaming properties and digestibility of yeast protein. *J. Food Sci.* **1987**, *52*, 1684–1688.

Ikai, A.; Fish, W. W.; Tanford, C. Kinetics of unfolding and refolding of proteins. *J. Mol. Biol.* **1973**, *73*, 165–184.

Kato, A.; Takahashi, A.; Matsudomi, N.; Kobayashi, K. Determination of foaming properties of proteins by conductivity measurements. *J. Food Sci.* **1983**, *43*, 62–65.

Kim, S. H.; Kinsella, J. E. Surface activity of food proteins: Relationships between surface pressure development, viscoelasticity of interfacial films and foam stability of bovine serum albumin. *J. Food Sci.* **1985**, *50*, 1526–1530.

Mita, T.; Nikai, K.; Hiraoka, T.; Matsuo, S.; Matsumoto, H. Physicochemical studies on wheat protein foams. *J. Colloid Interface Sci.* **1977**, *59*, 172–178.

Mita, T.; Ishida, E.; Matsumoto, H. Physicochemical studies on wheat protein foams: Relationship between bubble size and stability of foams prepared with gluten and gluten components. *J. Colloid Interface Sci.* **1978**, *64*, 143–153.

Monsalve, A.; Schechter, R. S. The stability of foams: Dependence of observation on the bubble size distribution. *J. Colloid Interface Sci.* **1984**, *97*, 327–335.

Mussellwhite, P. R.; Kitchener, J. A. The limiting thickness of protein films. *J. Colloid Interface Sci.* **1967**, *24*, 80–83.

Nishioka, G. M. Stability of mechanically generated foams. *Langmuir* **1986**, *2*, 649–653.

Nishioka, G. M.; Ross, S. A new method and apparatus for measuring foam stability. *J. Colloid Interface Sci.* **1981**, *81*, 1–7.

Oortwijn, H.; Walstra, P. The membranes of recombined fat globules: II. Composition. *Neth. Milk Dairy J.* **1979**, *33*, 134–154.

Phillips, M. C. Protein conformation at liquid interfaces and its role in stabilizing emulsions and foams. *Food Technol.* **1981**, *35*, 50–57.

Rha, C. K.; Pradipasena, P. Viscosity of proteins. In *Functional Properties of Food Macromolecules*; Mitchell, J. R., Ledward, D. A., Eds.; Elsevier Applied Science: London, 1986; pp 79–120.

Ross, S. Bubbles and foam. *Ind. Eng. Chem.* **1969**, *61*, 48–57.

Song, K. B.; Damodaran, S. Structure-function relationship of proteins: Adsorption of structural intermediates of bovine serum albumin at the air-water interface. *J. Agric. Food Chem.* **1987**, *35*, 236–241.

Waniska, R. D.; Kinsella, J. E. Surface properties of β-lactoglobulin: Adsorption and rearrangement during film formation. *J. Agric. Food Chem.* **1985**, *33*, 1143–1148.

Wright, D. J.; Hemmant, J. W. Foaming properties of protein solutions: Comparison of large-scale whipping and conductimetric methods. *J. Sci. Food Agric.* **1987**, *41*, 361–371.

Received for review February 9, 1991. Accepted May 13, 1991.